forests

MDPI

Article

Influence of *Chrysoporthe deuterocubensis* Canker Disease on the Physical and Mechanical Properties of *Eucalyptus urograndis*

Rasdianah Dahali [1], Paridah Md. Tahir [1,*], Adlin Sabrina Muhammad Roseley [2,*], Lee Seng Hua [1,*], Edi Suhaimi Bakar [2], Zaidon Ashaari [2], Mohd Redzuan Abdul Rauf [3], Nur Aziera Zainuddin [1] and Noor Syazwani Mansoor [2]

1 Institute of Tropical Forestry and Forest Products (INTROP), Universiti Putra Malaysia, Serdang 43400, Selangor, Malaysia; rasdianahdahali@gmail.com (R.D.); nurazierazainuddin@gmail.com (N.A.Z.)
2 Faculty of Forestry and Environment, Universiti Putra Malaysia, Serdang 43400, Selangor, Malaysia; edisuhaimi@upm.edu.my (E.S.B.); zaidon@upm.edu.my (Z.A.); mnoorsyazwani@gmail.com (N.S.M.)
3 Sabah Softwoods Berhad, Tawau 91019, Sabah, Malaysia; redzuan.abdulrauf@gmail.com
* Correspondence: parida@upm.edu.my (P.M.T.); adlin@upm.edu.my (A.S.M.R.); lee_seng@upm.edu.my (L.S.H.)

Abstract: *Eucalyptus* hybrid has been planted rigorously in wet tropical regions including Malaysia. Recently, there was a report on the occurrence of stem canker on these trees. However, the extent of the infections by this stem canker is unknown. The aim of this study was to evaluate the influence of stem canker disease, *Chrysoporthe deuterocubensis*, on the physical and mechanical properties of 11-year-old *E. urophylla* × *E. grandis* or also known as *E. urograndis*. The samples were taken from infected and healthy trees that were segregated into different classes based on the severity of the attack, i.e., healthy (class 1), moderately infected (class 2), severely infected (class 3) and very severely infected (class 4). A total of 1440 samples from four infection classes were used in this study. The physical and mechanical properties were determined according to the standard test procedures specified by the International Organization for Standardization (ISO) 13061:2014 (Parts 1 to 4, 13, 14 and 17) and British Standard (BS 373: 1957). From the result, a significant effect by the infection classes was observed on physical and mechanical properties of *E. urograndis*. All infected wood experienced less shrinkage compared to that of a healthy one, particularly the volumetric (Vol_{sh}) and radial shrinkage (R_{sh}). Wood from class 2 and class 3 was less affected by the infection while the majority of wood from class 4 had significantly lower density and poorer strength. Based on the strength data, wood from infection class 2 can be considered to be used for non-structural applications such as furniture, interior finishing, window frames and doors since reduction in mechanical properties was observed. Wood from class 3 would need further investigation to examine its suitability for structural applications.

Keywords: wet tropical; infections class; *Eucalyptus urograndis*; physical; mechanical properties

Citation: Dahali, R.; Md. Tahir, P.; Roseley, A.S.M.; Hua, L.S.; Bakar, E.S.; Ashaari, Z.; Abdul Rauf, M.R.; Zainuddin, N.A.; Mansoor, N.S. Influence of *Chrysoporthe deuterocubensis* Canker Disease on the Physical and Mechanical Properties of *Eucalyptus urograndis*. *Forests* **2021**, *12*, 639. https://doi.org/10.3390/f12050639

Academic Editor: Donald L. Rockwood

Received: 31 March 2021
Accepted: 14 May 2021
Published: 19 May 2021

1. Introduction

Currently, *Acacia mangium* Willd. is the main tree species being planted in Malaysia with a total planted area of approximately 300,000 hectares. However, for the past 10 years, *A. mangium* plantations have been affected by several diseases; the most serious being heart rot, gall rust and fast-spreading stem wilt-canker caused by *Ceratocystis* spp. *Ceratocystis* emerged as a new disease threat to *A. mangium* plantations in 2010 causing a serious mortality of young trees [1]. The most recent case reported was the infection of *Ceratocystis* in *A. mangium* plantations in Sabah, North Borneo, which have become one of the reasons for *Eucalyptus* being promoted as replacement for *A. mangium*. Owing to this adversity, one of plantations located in eastern Sabah where *Ceratocystis* has suffered severe damage,

and has switched from planting *A. mangium* to *Eucalyptus pellita* F. Muell [1]. The same situation was also experienced in Sumatra and Kalimantan, Indonesia, which switched from planting *A. mangium* to *E. pellita* [2,3]. *Eucalyptus* is an alternative tree species to *A. mangium* due to their fast growth, short rotation time, suitability of wood properties to many products, huge variability, high productivity, suitability to vegetative propagation [4] and high density value [5].

Eucalyptus species, as well as hybrids, have attracted interests from many countries thus have becoming a significant trait of global hardwood forestry industry. These species are cultivated in tropical (dry and wet), subtropical and temperate regions and comprise the most large-scale hardwood plantations throughout the world, estimated to occupy over 20 million hectares [6] with commercial plantations reaching over 90 countries [7,8]. In recent years, there has been a growing interest by the timber industry in using this resource as they may have the potential to ensure a sustainable supply of raw materials for different structural and non-structural products such as sawn timber [9], plywood [10], laminated timber [11,12], paper and pulp products [13,14]. Despite the promising prospect shown by *Eucalyptus*, these trees succumb to fungal diseases that originate from their native or introduced environments. Based on studies in other countries [15–17], the *Eucalyptus* spp. is susceptible and vulnerable to disease infection. Stem canker caused by genus *Crysoporthe* Gryzenh. and M. J. Wingf. are currently one of the most damaging diseases of *Eucalyptus* plantations in many tropical and subtropical region throughout the world [18–20]. Some plantations in Sabah have shown susceptibility of *E. pellita* to *Chrysoporthe deuterocubensis* Gryzenh. and M. J. Wingf., one of the most important pathogens that cause severe canker and tree death of *Eucalyptus* plantations in Malaysia [1,21,22]. The severity of infection may vary according to the infection period and the aggressiveness of the fungus [23]. Fungal infection can become serious and destroy a large area if there has been no prevention at the early stage [24]. Earlier experiences in Malaysia have seen many *Eucalyptus* plantation areas being wiped out due to this disease which has resulted in a drastic temporary slowdown of plantations development in the country [25]. The extent of distribution and virulence of this disease causes the greatest negative impact on *Eucalyptus* trees both in native and introduced ranges [26–28].

Chrysoporthe deuterocubensis has been identified as highly pathogenic to *Eucalyptus* species. Although trees die only in severe cases of disease, the impact of stem canker disease caused by Cryphonectriaceae in the forest industry can be devastating. It can disrupt the growth performance of the tree, reducing the volume and the quality of timber to the extent that it cannot be used for lumber or veneer-based products [29–31]. In addition, the wood is stained with kino/gummosis exudation from the cracks on the canker area [20,29,31] decreasing the value of the timber products. Since many *Eucalyptus* wood from these plantations is mainly being managed to produce woodchips [32], the effects of *C. deuterocubensis* infection on its properties seems less important. However, study of the effects *C. deuterocubensis* infection on the wood properties is crucial particularly for *Eucalyptus* hybrids like *E. urograndis* (*E. grandis* W. Hill ex Maiden × *E. urophylla* S.T. Blake) which have been planted extensively in China, South America and other parts of the world including Malaysia for higher value products such as sawn timber and wood veneers.

Moreover, it is vital to investigate the extent of damages in wood quality caused by *C. deuterocubensis* stem canker diseases so that the alternative application of the infected tree can be determined. The purpose of this study is to evaluate the effects of stem canker, *C. deuterocubensis*, on the physical and mechanical properties of *E. urograndis* wood.

2. Materials and Methods

2.1. Formulation of Disease Severity Classes

The *Eucalyptus* hybrids clone used in this study were identified as *E. grandis* x *E. urophylla* of Chinese origin, and is denoted as *E. urograndis*. An *E. urograndis* plantation plot located in Block 38 C (4°33′16.3″ N, 117°42′ 58.7″ E), Sabah Softwoods Berhad, Tawau, Malaysia, was surveyed in order to identify trees infected by *C. deuterocubensis*. The selected plot

is about 11.7 ha. This plot comprised 1908 standing trees of 11-year-old *E. urograndis* with three types of spacing (1.5 × 3, 1.8 × 3 and 3 × 3 m). The infected trees were identified and the pathogen that attack the trees was confirmed by a forest pathologist [22] through visual examination. Pictures were taken, the characteristics of the infection were recorded, and the extent of the infection was determined based on the severity of the symptoms occurred. Based on careful examinations of the pictures, as well as the physical symptoms/characteristics of the disease and its percentage of occurrence, the infected trees were grouped into four classes according to the severity of the infection (Table 1 and Figure 1).

Table 1. Severity classes for *Eucalyptus urograndis* infected by *Chrysoporthe deuterocubensis*.

Severity Classes	Category	Symptom [1]	Reference in Figure 1
1	Healthy	Stem appears normal without any symptom of being infected	a
2	Moderate	Swollen bark (callus)	b
		Cracking	c
		Fruiting structure	d
		Fresh kino pocket	e
		Canker	g
3	Severe	Swollen bark (callus)	b
		Cracking	c
		Fruiting structure	d
		Fresh kino pocket & fresh kino/gummosis	e & f
		Canker	g
		Sunken	j
		Rotten	k
4	Very severe	Swollen bark (callus)	b
		Cracking	c
		Fruiting structure	d
		Dried kino pocket & dried kino/gummosis	h & i
		Canker	g
		Sunken	j
		Rotten	k
		Shoot	l

[1] Visible characteristics on the standing tree.

2.2. Selection of Infected Tree

The infected trees were identified based on the appearance of canker symptoms on its stem. The selection of sample trees was made according to a rubric of stem canker symptoms (see Table 1) that was developed prior to the sampling. Selected trees were inspected visually to identify their symptoms and severity and then were assigned into different severity classes as listed in Table 1. Due to the limited number of infected trees in the chosen plot, only 8 trees were chosen as two trees were felled for each infection class. The logs were numbered and end coated, then brought to a processing workshop for further assessment.

Figure 1. Symptoms of *Cryphonectria deuterocubensis* on *E. urograndis*; (**a**) healthy tree, absence of any symptom; (**b**) swollen/callus, the reaction from the infected trees can be observed by the form of callus around the site of infection, leading to the bulging of the outer layer of bark; (**c**) cracking, by the shredding of outer layer bark, and these swollen/callus may coalesce to form a larger crack; (**d**) fruiting structure, stromata harbouring the fruiting bodies of *C. deuterocubensis* may develop in the bark and cambium of the cankers which are a clear sign of a *E. urograndis* infection; (**e**,**h**) kino pocket, due to injury of the cambium which resulting in the formation of kino pocket under the bark of infected stem; (**g**) canker, *C. deuterocubensis* causes perennial necrotic lesions (cankers) on the bark of stems are orange to reddish-brown on the surface; (**f**,**i**) fresh and dried kino/gummosis, as a defense response by the tree to infection of fungal disease, leads to abundant kino exudation produced from the secretory cells in the tree; (**j**) sunken, when the cambium is killed, the bark sinks inwards, giving the canker a characteristic sunken appearance; (**k**) rotten, decayed and brittle texture near the canker area due to repeated infections for a long period of time; (**l**) epicormic shoots, observed below the canker area as trees regrow after coppicing or pollarding.

2.3. Material Preparation

Each log was cut into several 1.5 m long billets and then coded and marked according to the position along the tree. Five billets of 1.5 m were obtained from the bottom part of the stem of each felled log as it contained the most obvious infected area of stem canker. The remaining logs were excluded from this study because there were very few defects (almost defect-free) present. A total of 40 billets were obtained from the 8 trees felled in this study. Using a Wood-Mizer twin vertical saw with a bank of four horizontal resaws (Wood-Mizer Europe, Koło, Poland), four to five 28 mm-thick boards were cut from each of the billets by using a live sawing technique (Figure 2).

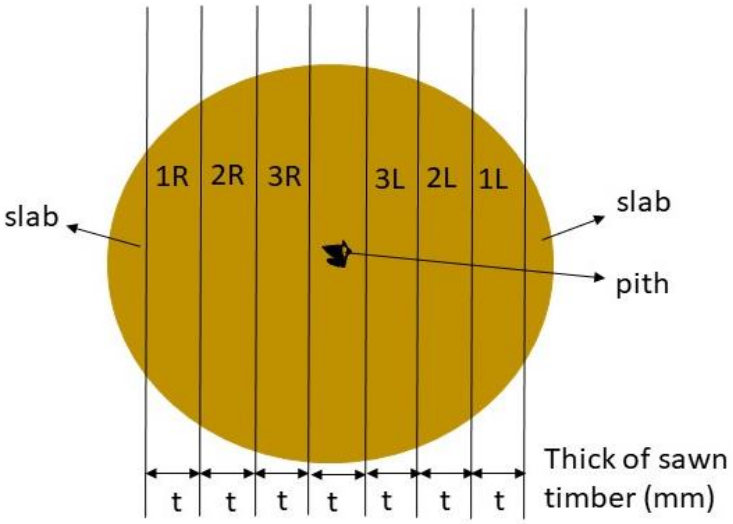

Figure 2. Cutting of infected logs by using live sawing technique. The numbering of 1R, 2R, 3R, 1L, 2L, 3L indicate the number and position (right (R) and left (L)) of boards obtained during sawing. The number of boards obtained depends on the diameter size of the log.

The initial moisture content of the boards was determined prior to air drying. The air drying was carried out under the shade at an average temperature of 32 °C and relative humidity (RH) of 82% until the boards reached <20% moisture content. After air dried, each board was planed and ripped into 150 × 20 × 20 mm strips. The strips (hereafter referred to as test samples) were then conditioned in a conditioning room maintained at 20 ± 2 °C and RH 65 ± 2% until a constant weight was achieved. Constant weight is reached when the weight of the sample does not differ by more than 0.2% between two successive weighings that were carried out at a minimum interval of 8 h.

The number of test samples used in the study varied according to the property being tested (Table 2).

Table 2. Size and number of test samples for physical and mechanical tests according to respective standards.

Property	Dimensions, mm ($t \times w \times l$)	No. of Samples [1]	Reference Standard
Initial/green moisture content (MC)		72	
Air-dry MC	20 × 20 × 20	168	ISO 13061-1
Equilibrium moisture content (EMC)		120	
Density	20 × 20 × 20	120	ISO 13061-2
Tangential shrinkage (T_{sh})			ISO 13061-13
Radial shrinkage (R_{sh})	20 × 20 × 20	120	
Volumetric shrinkage (Vol_{sh})			ISO 13061-14
Modulus of rupture (MOR)	20 × 20 × 320	120	ISO 13061-3

Table 2. *Cont.*

Property	Dimensions, mm ($t \times w \times l$)	No. of Samples [1]	Reference Standard
Modulus of elasticity (MOE)	20 × 20 × 320		ISO 13061-4
Shear ($S_{//}$ and $S_{\perp}$)	20 × 20 × 20	240	ISO 3347
Compression ($Com_{//}$ and $Com_{\perp}$)	20 × 20 × 60	240	ISO 13061-17
Hardness (H_t and H_r)	20 × 20 × 60	240	BS 373

[1] Total number of samples for four infectation classes.

2.4. Evaluation of Physical Properties

2.4.1. Moisture Content

The moisture content of the lumbers was determined at three conditions: initial (green), air-dry and equilibrium moisture content (EMC) at 12%. The moisture content (MC) was determined according to Equation (1);

$$\text{Moisture content, MC (\%)} = 100\ (W_2 - W_1)/W_1 \quad (1)$$

where W_1 is the oven-dry (OD) weight (g) of the samples, and W_2 is the weight (g) of the samples either in green (after sawing), after air-dried, or after conditioned at 12% EMC.

2.4.2. Density

The density of the wood was determined according to Equation (2);

$$\text{Density, } \rho\ (\text{kg/m}^3) = (Wi/Vi) \quad (2)$$

where *Wi* is the air-dried (AD) weight of the samples (g) and *Vi* is the air-dried (AD) volume of the samples after reconditioning (cm^3).

The density at 12% moisture content ($\rho 12$) was calculated by applying Equation (3).

$$\rho_{12} = \rho_W \frac{1 + 0.01(12 - W)}{1 + 0.01(12 - W)\frac{\rho_W}{\rho_{H_2O}}} \quad (3)$$

where W is the moisture content at the time of test (%) and ρH_2O is the density of water, 1 g/cm^3.

2.4.3. Shrinkage

Measurement points were marked at the center of the radial and tangential surfaces of test samples. The dimension in tangential direction was measured by placing a digital caliper (Mitutoyo, Kanagawa, Japan) at the center point of the radial surfaces, whilst the measurement of radial dimension was taken at the center point of the tangential surfaces. All measurements were taken at the same point during each stage of moisture conditions.

Since the moisture content of the test samples were below the fiber saturation point (FSP), the samples were soaked in distilled water at (20 ± 2) °C until no further change in dimensions had occurred. The dimensions of the test samples were measured between the marks prior to soaking and at each stage of moisture conditions. The wet samples were wiped dry prior to measuring the radial (I_{r1}) and tangential (I_{t1}) dimensions to an accuracy of 0.02 mm. Subsequently, they were placed in an oven at 103 ± 2 °C until they reached a constant weight. The samples were cooled in a desiccator, then the dimensions were measured to an accuracy of 0.02 mm (obtaining I_{r2} and I_{t2}). The linear shrinkage (T_{sh} and R_{sh}) and volumetric shrinkage (V_{sh}) of the samples were determined by Equations (4)–(6), respectively.

$$T_{sh} = 100\ (I_{t1} - I_{t2})/I_{t1} \quad (4)$$

$$R_{sh} = 100\ (I_{t1} - I_{r2})\ I_{r1} \quad (5)$$

$$V_{sh}(\%) = 100\ (I_{r1} \times I_{t1}) - (I_{r2} \times I_{t2})/(I_{r1} \times I_{t1}) \quad (6)$$

where I_{r1} and I_{t1} are the dimensions (mm) of the green or fully saturated test sample, measured in the radial and tangential direction, respectively.

I_{r2} and I_{t2} are the dimensions (mm) of the test sample at absolute dry (oven-dry) condition, measured in the radial and tangential direction, respectively.

2.5. Evaluation of Mechanical Properties

ISO standards [33,34] were the main testing standards used in this study except for the hardness test. Since the diameters at breast height (dbh) of the 11-year-old *E. urograndis* were rather small with an average of 32 cm, limited number of samples could be cut from each log. As ISO 13061-12: Determination of Static Hardness requires larger size (50 × 50 × 50 mm) test samples, BS 373 [35] was used as it requires smaller size.

All tests for the mechanical properties were conducted using a Universal Testing Machine (Instron 5567, Norwood, MA, USA) with a loading capacity of 100 kN. Following the test, the types of the failure mode of the static bending samples were visually examined and classified according to American Society for Testing Materials (ASTM) D-143 [36]. The strength (modulus of rupture, MOR) and stiffness (modulus of elasticity, MOE) in static bending, compression parallel and perpendicular to the grain ($Com_{//}$ and $Com_{\perp}$), shear parallel and perpendicular to the grain ($S_{//}$ and $S_{\perp}$) and surface hardness in tangential and radial direction (H_t and H_r) were determined using Equations (7)–(11), respectively:

$$\text{Bending, MOR (MPa)} = 3P_{max}\ L/2bh^2 \quad (7)$$

where P_{max} is the maximum load (MPa), L is the span (mm), b is the breath of the test sample (mm), and h is the height of the test sample (mm).

$$\text{Bending, MOE (GPa)} = PL^3/4bh^3f \quad (8)$$

where P is the load equal to the difference between the upper and lower limits of loading (GPa), L is the length of the span (mm), b is the breath of the test sample (mm), h is the height of test sample (mm) and f is the deflection which corresponds to the proportional limit (mm).

$$\text{Compression, } Com_{//} \text{ and } Com_{\perp} \text{ (MPa)} = F_{max}/a \times b \quad (9)$$

where F_{max} is the maximum load (MPa) and a × b is the cross-sectional dimension of wood samples (mm^2).

$$\text{Shear, } S_{//} \text{ and } S_{\perp} \text{ (MPa)} = P/bh \quad (10)$$

where P is the load at maximum limit proportionality (MPa), b is the breath of test sample (mm) and h is the height of test sample (mm).

$$\text{Hardness, } H_t \text{ and } H_r \text{ (kN)} = K \times F \quad (11)$$

where F is the maximum load during the penetration of the plunger into the test sample to the specified depth in newtons and K is the coefficient equal to 1 and 4/3 in the case of penetration of the plunger to a depth of 5.64 mm and 2.82 mm, respectively.

All the strengths were adjusted to 12% moisture content according to the calculations provided in the respective standards.

2.6. Statistical Analysis

The data were analysed and interpreted using one-way analysis of variance (ANOVA) to evaluate the effects of infection classes on the physical and mechanical properties of the wood. The differences between the mean values of each severity classes were further tested using Duncan's multiple range (DMR) test at $\alpha \leq 0.05$. Pearson's correlation coefficients

were calculated to evaluate the relationships between infection classes and density, as well as with MOR and MOE of the infected wood. All statistical analyses were conducted using SPSS version 22.0 (IBM, Armonk, NY, USA).

3. Results and Discussion

3.1. Visual Defects on the Lumber

Limited numbers of 28 mm-thick lumbers were obtained from the felled logs as the diameter of the logs is rather small (25–38 cm). Four to five pieces of 28 mm-thick lumber were obtained from each log from class 1 and 2, whilst only four pieces from class 3 and 4. Defects such as surface checks, kino pocket, gummosis, decay and end splits were observed in the majority of the lumbers, particularly pieces obtained from the first cut (mostly sapwood layer) except for lumbers obtained from class 4. The infected area in class 4 was much higher and deeper compared to class 2 and 3. As shown in Figure 3, lumber taken from healthy trees (class 1) was almost free from any defect except for some tight knots. Swollen bark (callus), cracks, fruiting structure and kino pocket appeared on lumbers taken from class 2 (Moderate). In class 3 (Severe), the kino pockets increased in number where some were filled with gums (also known as gummosis or resinosis) as the infection appeared more severe. The most severe symptom was found in class 4 (Very severe) where a large section of the stem started to soften indicating the beginning of decay.

Figure 3. Some of the defects found on the surface of lumbers cut from different infection classes: Class 1, no apparent defect except for tight knots; Class 2, arrow showing a kino pocket; Class 3, arrow showing kino pocket filled with kino/gummosis; Class 4, area in the rectangular showing signs of decay.

3.2. Effects of Chrysoporthe deuterocubensis Infection on Physical Properties of Eucalyptus urograndis Wood

Table 3 gives the summary of ANOVA for the effects of infection classes on the physical strength of 11-year-old *E. urograndis*. With the exception of air-dry moisture content and tangential shrinkage (T_{sh}), all physical properties were significantly affected by the level of infection. The moisture contents (initial, air-dry and EMC), density, volumetric shrinkage (Vol_{sh}), tangential shrinkage (T_{sh}) and radial shrinkage (R_{sh}) of healthy and infested 11-year-old *E. urograndis* trees are presented in Table 4. Interestingly, irrespective of drying conditions, the moisture content of wood from healthy trees is relatively higher than those from infected trees. The wood moisture content decreased as the level of infections became more severe. One week after felling, the average initial MC of the lumbers differed

significantly ($p \leq 0.01$) among infection classes. Nonetheless, no significant reduction was observed in air-dry moisture content of wood which may be ascribed to the effects of weathering. The equilibrium moisture content (EMC) of the wood that had been conditioned at 20°C and 65% relative humidity (RH) did not vary significantly between classes 1, 2 and 3 (10.1% to 10.5%). However, EMC of class 4 wood was significantly lower (9.7%) compared to other classes.

Table 3. Summary of analysis of variance (ANOVA) for the effect of infection by *Crysoporthe deuterocubensis* on the physical properties of *Eucalyptus urograndis* lumbers.

Source	MC (%)			Density (kg/m^3)	Vol_{sh} (%)	T_{sh}(%)	R_{sh} (%)
	Initial	Air-Dry	EMC				
Degree of freedom (*df*)	3	3	3	3	3	3	3
Sum of Squares (SS)	3589.3	7.8	10.5	458,806.4	465.3	14.4	43.3
Mean SS	1196.4	2.6	3.5	152,935.5	4.0	4.8	14.4
p-value	0.000 ***	0.118	0.000 ***	0.000 ***	0.000 ***	0.111	0.002 **

Note: ** high significance ($p < 0.01$); *** very high significance ($p < 0.001$). MC, moisture content; EMC, equilibrium moisture content; Vol_{sh}, volumetric shrinkage; T_{sh}, Tangential shrinkage; R_{sh}, radial shrinkage.

Table 4. Effects of infection by *Crysoporthe deuterocubensis* on physical properties of *Eucalyptus urograndis* lumbers [1].

Infection Classes	Value	MC (%) [2]			Density [3] (kg/m^3)	Vol_{sh} (%)	T_{sh} (%)	R_{sh} (%)
		Initial	Air-Dry	EMC				
1	Mean [4]	105.4 [a]	16.3 [a]	10.5 [a]	670.8 [a]	15.1 [a]	9.1 [a]	6.8 [a]
(Healthy)	SD	6.0	0.8	0.6	80.7	4.1	1.3	2.3
2	Mean	101.4 [b]	16.2 [a]	10.1 [b]	618.9 [b]	14.0 [b]	8.4 [a]	6.1 [a]
(Moderate)	SD	8.0	1.2	0.6	85.9	1.94	1.7	1.47
3	Mean	98.8 [c]	16.2 [a]	10.2 [ab]	706.8 [a]	14.5 [ab]	8.8 [a]	6.3 [a]
(Severe)	SD	14.2	1.4	0.7	106.6	2.0	1.7	1.32
4	Mean	84.4 [d]	15.4 [a]	9.7 [c]	542.3 [c]	12.9 [c]	8.1 [a]	5.1 [b]
(Very severe)	SD	8.7	1.1	0.7	60.4	1.8	1.3	1.8
p-Value		0.000 ***	0.118	0.000 ***	0.000 ***	0.000 ***	0.111	0.002 **

Note: ** high significance ($p < 0.01$); *** very high significance ($p < 0.001$). [1] SD, standard deviation; MC, moisture content; Vol_{sh}, volumetric shrinkage; T_{sh}, Tangential shrinkage; R_{sh}, radial shrinkage. [2] Initial condition refers to conditioning of logs (green) after felling; Air-dry condition refers to lumbers that were dried under the shade (average temperature: 32 °C; RH 84%); EMC condition refers to conditioning of test samples after adjusted to 12% EMC. [3] Density after being adjusted to 12% moisture content. [4] Means followed by the same letter in the same column are not significantly different at $\alpha = 0.05$ according to Duncan multiple range test.

The results suggest that significant amounts of woody tissues had been attacked by *C. deuterocubensis* so much so it dried up the tissues, a sign of early degradation. As fungus penetrates into tree bark, it colonizes the phloem (tissue responsible for transporting the nutrients), then penetrates into the vascular cambium, and finally reaches the xylem (tissue that responsible for transporting water to other parts of the tree) [37]. If the attacks continue and spread to other parts of the wood, it would disrupt tree growth activities thus causing loss of moisture, as well as exposing the wood to other biodegradable agents such as fungi or bacteria. In the case of severe attack, the wood would be softened and rotten/decayed as a result of nutrients deficiency, leading to decline in tree canopy with the infected tree eventually dying.

The density of *E. urograndis* appears not to be affected by the disease except for class 2 (moderate) and class 4 (very severe). The density ranged from 542.3 ± 60.4 to 706.8 ± 106.6 kg/m^3; the lowest being those from class 4 indicating a substantial amount of degradation have occurred within the woody cells. As mentioned by Alfenas et al. [38], *E. urograndis* infected by *Ceratocystis* have reduced growth of tree and the volumetric of

wood and thus it indirectly reduced the density of wood. This finding was similar to those of Mafia et al. [23] and Fernandes et al. [39] who reported that wood from both *E. grandis* hybrid and *E. urophylla* clones infected by *Ceratocystis* has lower density than those from healthy trees.

The shrinkage behavior of hybrid *E. urograndis* can be seen in Table 4. The Vol_{sh}, T_{sh} and R_{sh}values were in the ranges of 12.9–15.1%, 8.2–9.1% and 5.1–6.8%, respectively. These values are similar to other *Eucalyptus* clones and hybrids obtained by several researchers [40–44]. These studies also reported higher T_{sh} percentage than R_{sh}. In this study, the Vol_{sh}, T_{sh} and R_{sh} of infected samples were lower than those of the healthy ones. Class 4 recorded significantly lower values in terms of Vol_{sh} and R_{sh} compared to the other 3 classes. Meanwhile, Vol_{sh}, T_{sh} and R_{sh} of class 3 did not differ significantly to both class 1 and class 2. Gunduz et al. [37] reported similar findings in their study using chestnut tree infected by *Cryponectria parasitica* (Murrill) M.E.Barr as the shrinkage of healthy wood was higher than that from infected trees. As mentioned earlier, wood from healthier trees contains higher moisture and nutrients for tree growth, thus tends to shrink more than that from less healthy trees.

The shrinkages of wood from class 4 were generally lower than the other classes, particularly radial shrinkage (R_{sh}). A similar result was found in a study by Wessel et al. [41], who reported that R_{sh} is easily influenced by external factors such as cracks or checks during drying. In addition, the growth of chlamydospores of *Crysoporthe* spp. that enter the wood through wound or injuries might also lead to the formation of cracks in the wood. According to Schwarze et al. [45], chlamydospores germinates and forms a mass of interwoven hyphae called mycelium or a mycelial mat that could mechanically induced radial cracks in the infected tree. Hence, due to the earlier existence of cracks, when exposed to moisture, the extent of radial shrinkage is much less compared to healthier wood (class 1). Another plausible reason for this kind of behavior is that the infected samples contained a lower amount of holocellulose, subsequently the cell walls contained fewer free hydroxyl groups and water molecules (as seen in lower moisture content percentage in all infected wood) to bind the cells [37]. The decrement of the holocellulose in the cell wall is a result of fungus consuming holocellulose as a nutrition source for the development of their colonization in wood [37,46].

In summary, disease caused by *C. deuterocubensis* did not have disastrous effects on the shrinkage properties of infected wood. Moreover, all infected wood experienced less shrinkage compared to that of healthy wood, particularly the volumetric (Vol_{sh}) and radial shrinkage (R_{sh}). The overall values of shrinkage in *E. urograndis* revealed that this species is rather dimensionally unstable with a moderate extent of shrinkage. This was in agreement with Acosta et al. [47] who stated that *Eucalyptus* wood is known as dimensionally unstable due to the variation of moisture content.

3.3. Effect of Chrysoporthe deuterocubensis Infection on Mechanical Properties of Eucalyptus urograndis Wood

Table 5 gives the summary of ANOVA for the effects of infection classes on the mechanical strength (adjusted to 12% moisture content) of 11-year-old *E. urograndis*. All the strength properties were significantly affected by the level of infection, in particular the MOR, MOE, Shear// H_t and H_r as indicated by the very low *p*-values. Interestingly, compression perpendicular to grain appears not to be affected by the level of infection. Wilcox [48] reviewed the effects of the early stages of decay on wood strength. The author found that the compression perpendicular to grain is the least affected properties by fungal decay. Only 5–6% loss was recorded as compared to toughness (50%), MOR and MOE (as much as 50% and 55% respectively depending on the weight loss and the type of fungi).

Table 5. Summary of ANOVA for the effect of infection by *Crysoporthe deuterocubensis* on the mechanical properties of *Eucalyptus urograndis* lumbers.

Source	MOR (MPa)	MOE (GPa)	$Com_{//}$ (MPa)	$Com_{\perp}$ (MPa)	$Shear_{//}$ (MPa)	$Shear_{\perp}$ (MPa)	H_t (kN)	H_r (kN)
Degree of freedom (*df*)	3	3	3	3	3	3	3	3
Sum of Squares (SS)	10,937.3	202.6	1387.4	161.5	78.1	285.7	40.7	29.9
Mean SS	3645.8	67.5	462.5	53.8	26.0	95.2	13.6	10.0
p-Value	0.000 ***	0.000 ***	0.001 **	0.252	0.000 ***	0.002 **	0.000 ***	0.000 ***

Note: ** high significance ($p < 0.01$); *** very high significance ($p < 0.001$). MOR, modulus of rupture; MOE, modulus of elasticity; $Com_{//}$ and $Com_{\perp}$, compression strength parallel and perpendicular to the grain; $Shear_{//}$ and $Shear_{\perp}$, shear strength parallel and perpendicular to the grain and H_t, hardness tangential and H_r, hardness radial.

As shown in Table 6, the MOR and MOE of the wood ranged from 85.4 to 114.1 MPa and from 10.6 to 13.9 GPa, respectively. Pima et al. [49] also reported that the MOR and MOE of 9-year-old *Eucalyptus* hybrid ranged from 72.6 to 108.5 MPa for MOR and 8.5 to 12.7 GPa for MOE. Except for class 3 (Severe), all infected classes showed a lower value of MOR and MOE than class 1. Wood from infection class 4 appears to be the weakest, having MOR of 85.4 MPa and MOE of 10.6 GPa which are respectively 18% and 20% lesser than those of class 1.

Table 6. Effects of infection by *Crysoporthe deuterocubensis* on mechanical properties of *Eucalyptus urograndis* lumber [1].

Infection Classes	Value	MOR (MPa)	MOE (GPa)	$Com_{//}$ (MPa)	$Com_{\perp}$ (MPa)	$Shear_{//}$ (MPa)	$Shear_{\perp}$ (MPa)	H_t (kN)	H_r (kN)
1 (Healthy)	Mean [2]	91.1 ^{ab}	12.3 ^{a}	49.5 ^{a}	14.4 ^{a}	7.1 ^{a}	18.8 ^{a}	5.6 ^{a}	5.5 ^{a}
	SD	16.7	2.2	8.5	2.8	1.3	4.4	1.4	1.2
2 (Moderate)	Mean	80.5 ^{bc}	10.8 ^{b}	50.8 ^{a}	16.6 ^{a}	7.9 ^{a}	14.6 ^{b}	5.5 ^{a}	5.1 ^{a}
	SD	19.4	1.8	6.6	7.8	1.4	4.2	1.5	1.1
3 (Severe)	Mean	96.4 ^{a}	12.7 ^{a}	50.1 ^{a}	12.7 ^{a}	7.7 ^{a}	15.3 ^{b}	6.0 ^{a}	5.1 ^{a}
	SD	24.3	2.7	12.3	5.2	1.5	5.1	1.1	0.7
4 (Very severe)	Mean	71.7 ^{c}	9.5 ^{c}	42.4 ^{b}	13.9 ^{a}	5.9 ^{b}	13.0 ^{b}	4.4 ^{b}	4.2 ^{b}
	SD	22.1	2.4	8.1	7.7	2.2	2.2	1.3	0.8

[1] SD, standard deviation; MOR, modulus of rupture; MOE, modulus of elasticity; $Com_{//}$ and $Com_{\perp}$, compression strength parallel and perpendicular to the grain; $Shear_{//}$ and $Shear_{\perp}$, shear strength parallel and perpendicular to the grain; H_t, and H_r, hardness tangential and hardness radial. [2] Means followed by the same letter in the same column are not significantly different at $\alpha = 0.05$ according to Duncan multiple range test.

The compressive strength parallel and perpendicular to the grain ($Com_{//}$ and $Com_{\perp}$) in this study ranged from 42.4 to 50.8 MPa and 12.7 to 16.6 MPa, respectively. No significant difference was found in compressive strength perpendicular to the grain. Infected wood from class 2 had higher $Com_{\perp}$ (by 13%) than those of class 1 whilst both classes 3 and 4 recorded lower values. Meanwhile, a significant difference was found in compressive strength parallel to the grain especially for the wood from class 4, which showed a reduction of 14.3% compared to class 1. In the case of shear strength parallel ($Shear_{//}$) and perpendicular to the grain ($Shear_{\perp}$), the values ranged from 5.9 to 7.9 MPa and 13.0 to 18.8 MPa, respectively. Similarly, wood from class 4 had the lowest shear values, which were, respectively, 17% and 31% lower than those of the values averaged for class 1. The hardness of *E. urograndis* in both directions, H_t and H_r, ranged between 4.4–6.0 kN and 4.2–5.5 kN, respectively. Among the infection classes, class 4 gives notably softer wood owing to a greater amount of infection that appears to affect the surface of the wood into becoming rotten as shown in Figure 1. Such an effect was found to be highly significant ($p \leq 0.01$) for all the strengths values, except for compression perpendicular to the grain, which was not significant ($p > 0.1$).

The lower strength in infected wood compared to the healthy one is the obvious symptom of the wood being decomposed by either fungi or bacteria. Fungi colonize wood and degrade cell wall components to form brown, white or soft rot. All of them degrade structural polymers of the wooden cell wall. Brown-rot fungi degrade primarily the carbohydrate components of wood and mainly leave the lignin undegraded. On the other hand, soft rot is preferential in degrading carbohydrates and a small portion of lignin while white rot degrades both carbohydrates and lignin. According to Blanchette et al. [50], the rate and extent of lignin, cellulose, and hemicellulose removal varies among species of fungi. For example, soft-rot fungi erode the secondary wall or form discrete cavities within the cell wall. Each type of decay has many forms which can be classified only by examining the microscopic and ultrastructural characteristics. These fungi reduce the strength of wood by metabolizing the holocellulose fraction. Many fungal diseases from ascomycetes species such as *Crysoporthe* and *Ceratocystis* attack the cellulose and hemicellulose [37,51]. Holocelluloses were the major component in wood which play an important role in the wood strength.

Fungi begin as fungal spores or mycelial fragments. Then, the spores germinate in the production, which are long, end-to-end cells of the fungus, fine hair-like structures known as fungal hyphae. Hyphae fragments landing on wood can also initiate growth, leading to broader colonisation of the wood. The hyphae of *C. deuterocubensis* spread through to the wound or crack and grow in the lumen of individual woody cells, usually after entering through a "pit" depression in the wall. During this early growth stage, all wood-inhabiting fungi seek out stored products in the parenchyma as a ready nutrient source for the fungus's energy, as well as to build up fungal biomass within or on the surface of the wood structure. Then, they move towards the vascular cambium and secondary xylem by destroying the tissue fibers and vessels in cell walls [23,37,52,53]. As a result, the strength of wood is weakened. Such symptoms were found to be marginal in wood from classes 2 and 3, but quite obvious in class 4. In all cases, there was no visual sign of the wood being attacked by the bacteria suggesting that the degradation caused by the fungi was still in its early stage.

Failure Modes in Bending Strength

Failure mode serves as indicator to predict the level of strength/grade of a material whilst the characterization of different types of failure help to explain the behavior of the wood upon loading. The typical failure modes exhibited by the healthy and infected samples when subjected to a static bending test can be seen in Figures 4–6. Meanwhile, the percentage of failure modes according to infection class is shown in Figure 7. Based on the appearance of the fractured surface, the types of failure observed in *E. urograndis* were simple tension, splintering tension, brash tension and compression. It was found that the most frequent failure occurred was simple tension (49%), followed by splintering tension (25%), compression (24%) and brash tension (2%). Simple tension occurs when a tensile stress parallel to the grain causes direct pulling into two parts of the wood on the underside of the sample. In a smooth, straight-grained sample, this is normal, particularly when the wood is seasoned. Meanwhile, splintering tension failure consists of a considerable number of slight tension failures, resulting in a ragged or splintery break on the underside of the beam. This is common in tough/densely woods. In this case, the fracture surface is fibrous. Simple tension and splintering tension are mainly caused by high density and low moisture content of the wood which usually gave a higher strength and elasticity values [54]. This can be seen clearly in the MOR and MOE values of samples having these two types of failure. As shown in Figures 5 and 6, samples that contained either simple tension or splintering tension recorded relatively higher MOR, 94.8 and 100.2 MPa, as well as higher MOE, 12.2 and 12.1 GPa, respectively. Samples having both brash and compression failures were consistently lower in strength and stiffness.

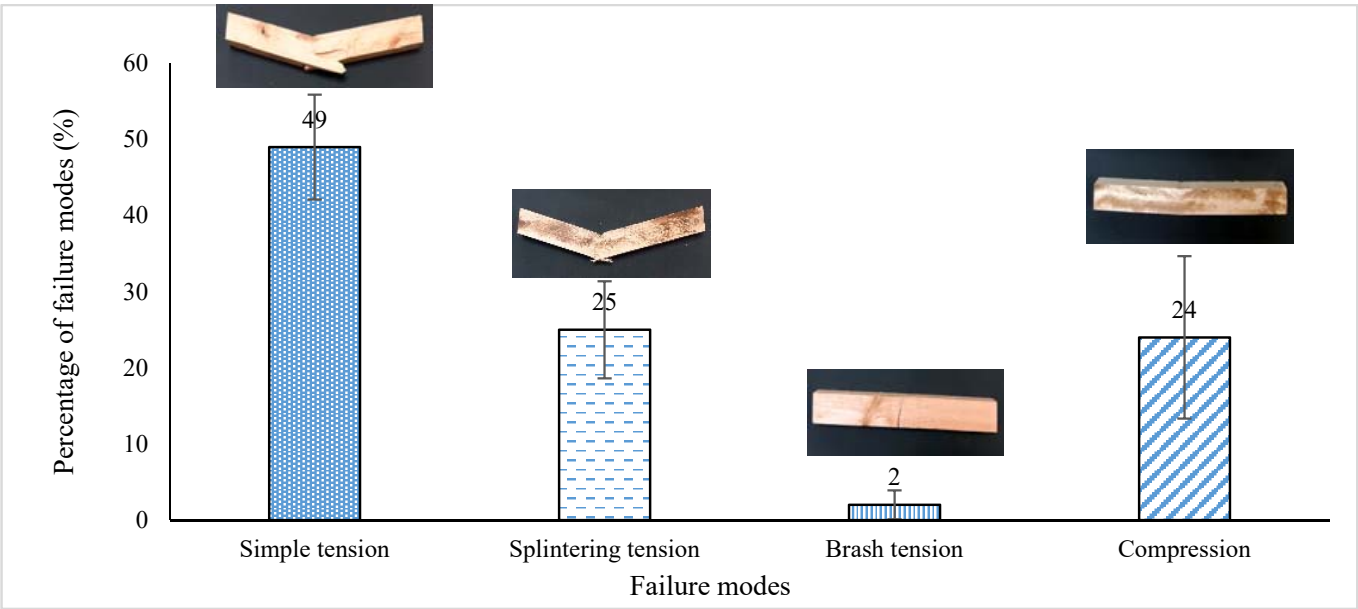

Figure 4. Types and percentage of occurrence of failure (in static bending) of *Eucalyptus urograndis*.

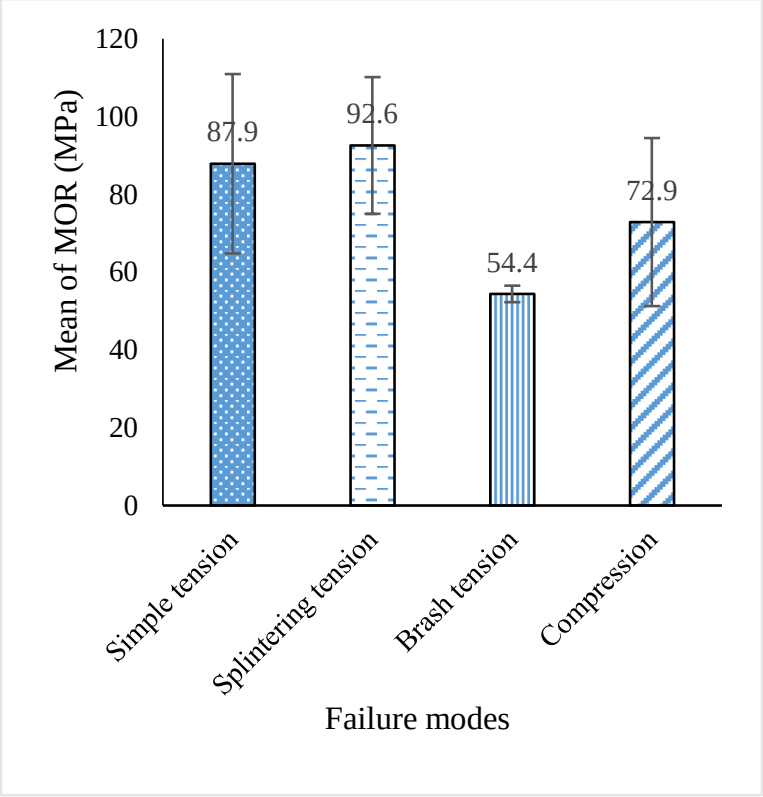

Figure 5. Average modulus of rupture (MOR) of *Eucalyptus urograndis* wood corresponding to types of failure.

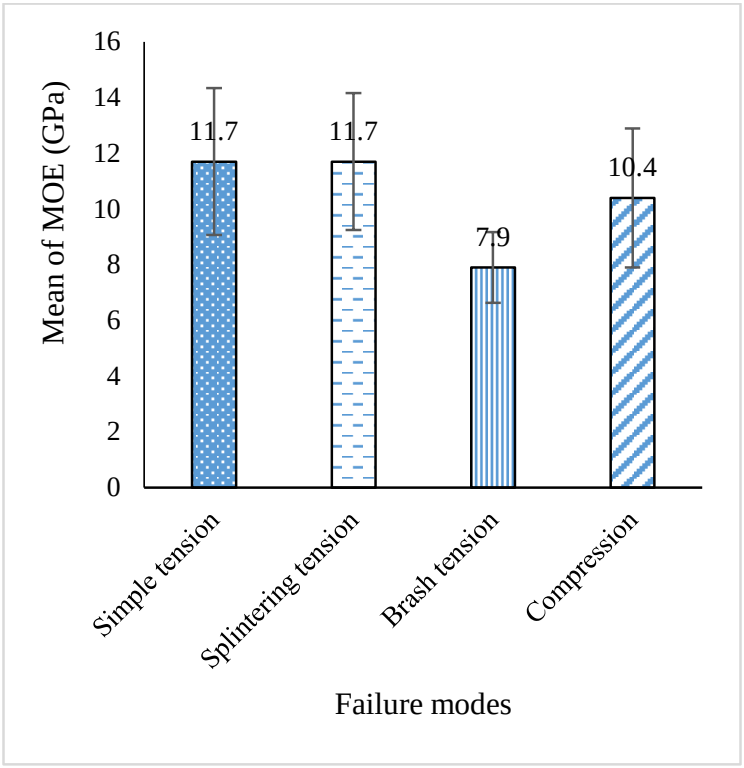

Figure 6. Average modulus of elasticity (MOE) of *Eucalyptus urograndis* wood corresponding to types of failure.

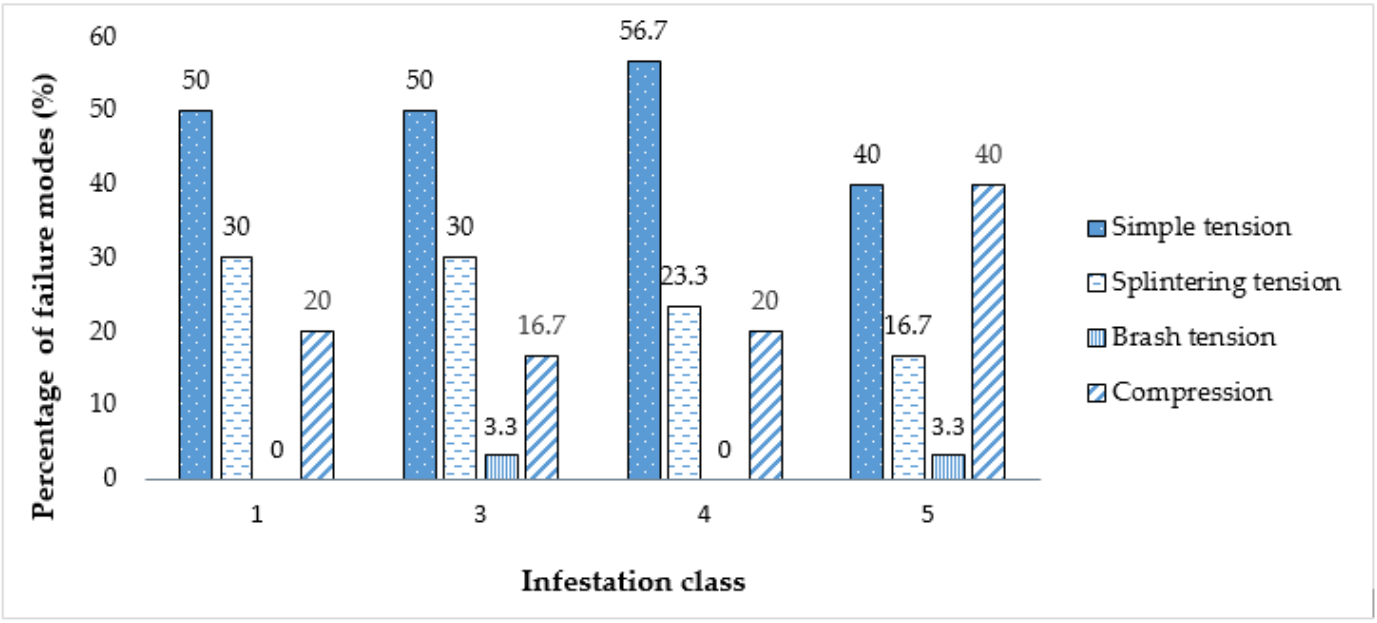

Figure 7. Percentage of failure modes according to infection class.

In this study, samples from infection classes 2 and 4 (moderate and very severe) were the only two classes experiencing failure in brash tension which was 3.3% each (Figure 7). Brash tension usually occurs when a sample fails with a clean break that extends entirely through. Brash tension is typically found in brittle wood, which gives way suddenly and without warning, like a piece of chalk. The surface of the fracture is described as brittle in this case. The sample from class 4 experienced the highest percentage of compression

failure (40%) while the other classes had 20% and less. Compression failure typically occurs in clear, low-density and green wood [54]. Usually, this type of failure starts on the top side shortly after the elastic limit is reached and progresses downward, sometimes almost to the neutral plane before complete failure occurs. Frequently, two or more failures occur at the same time. For example, tension breaks will eventually appear, so that both types of failure are present with completion of the test. Since the sample from class 4 was the most decayed sample and had relatively lower density (542.3 kg/m^3) and moisture content (9.7%), the wood from this class recorded higher brash tension and compression failure of 3.3% and 40%, respectively, compared to the other infected classes. The findings implied that the wood from class 4 was relatively weaker. Meanwhile, wood from classes 1, 2, and 3 were stronger as indicated by their higher wood density ($\geq$600 kg/m^3) and higher occurrence of simple tension ($\geq$50%). Hence, it can be construed that the infected wood from classes 2 and 3 were relatively sound and had good strength comparable to that of wood from the healthy (class 1) sample.

3.4. Correlation between Infection Class and Bending Strength

Pearson's correlation between infection class, MOR and MOE of *E. urograndis* wood was conducted. The correlation was weak but significant (p = 0.037) with MOE, but no significant correlation was obtained between severity classes and MOR (p = 0.152). Generally, both MOR and MOE decreased along with an increase in infection class/severity as indicated by the weak negative correlations of MOR (r = −0.132) and MOE (r= −0.191). The lower correlation coefficient may be triggered by the strange behavior of class 3 (severe), which exhibited somewhat higher mechanical strength compared to that of class 1 (healthy) and class 2 (moderate).

4. Conclusions

This study revealed that the physical and mechanical properties of 11-year-old *E. urograndis* wood were significantly affected by the level of infection by *C. deuterocubensis*. Physical and mechanical properties of the infected wood in class 1 (healthy), class 2 (moderate) and class 3 (severe) did not differ much. Only the properties of *E. urograndis* from infection class 4 (very severe) were significantly affected as relatively inferior properties were recorded. Generally, shrinkage properties of the infected wood were not affected negatively by the infection of *C. deuterocubensis*. Instead, all infected wood experienced less shrinkage compared to that of healthy one, particularly the volumetric (Vol_{sh}) and radial shrinkage (R_{sh}). Based on the strength data, wood from class 2 and class 4 experienced reductions of 11.6% and 21.3% in MOR while wood from class 3 had higher MOR than that of the class 1 (healthy). It is recommended that wood from class 2 could be used for non-structural application such as furniture, interior finishing, window frames and doors. As for wood from class 3, a more comprehensive study is needed to examine its suitability for structural applications despite its higher mechanical strength compared to that of the healthy trees.

Author Contributions: Conceptualization, P.M.T. and A.S.M.R.; Methodology, P.M.T., A.S.M.R., R.D. and M.R.A.R.; Formal Analysis, R.D. and L.S.H.; Investigation, R.D., N.A.Z. and N.S.M.; Data Curation, R.D., P.M.T. and Z.A.; Writing—Original Draft Preparation, R.D., L.S.H. and A.S.M.R.; Writing—Review and Editing, R.D., L.S.H. and P.M.T.; Supervision, P.M.T., A.S.M.R., L.S.H. and E.S.B.; Project Administration, P.M.T.; Funding Acquisition, P.M.T., A.S.M.R., L.S.H., E.S.B. and Z.A. All authors have read and agreed to the published version of the manuscript.

Funding: This research was funded by the Trans-disciplinary Fundamental Research Grant Scheme (TRGS 2018-1), Reference code: TRGS/1/2018/UPM/01/2/3 by Ministry of Higher Education (MOHE), Malaysia.

Data Availability Statement: Not applicable.

Acknowledgments: The authors would like to express their gratitude to Sabah Softwoods Berhad (SSB) for providing the wood materials, and to the Institute of Tropical forestry and Forest Prod-

ucts and Faculty of Forestry and Environment, Universiti Putra Malaysia for the facilities and assistance provided.

Conflicts of Interest: The authors declare no conflict of interest.

References

1. Lee, S.S. Observations on the successes and failures of acacia plantations in Sabah and Sarawak and the way forward. *J. Trop. For. Sci.* **2018**, *30*, 468–475. [CrossRef]
2. Tarigan, M.; Roux, J.; Van Wyk, M.; Tjahjono, B.; Wingfield, M.J. A new wilt and die-back disease of *Acacia mangium* associated with *Ceratocystis manginecans* and *C. acaciivora* sp. nov in Indonesia. *S. Afr. J. Bot.* **2011**, *77*, 292–304. [CrossRef]
3. Nambiar, E.K.S.; Harwood, C.E.; Mendham, D.S. Paths to sustainable wood supply to the pulp and paper industry in Indonesia after diseases have forced a change of species from acacia to eucalypts. *Aust. For.* **2018**, *81*, 148–161. [CrossRef]
4. Rezende, G.D.S.; de Resende, M.D.V.; de Assis, T.F. Eucalyptus breeding for clonal forestry. In *Challenges and Opportunities for the World's Forests in the 21st Century*; Springer: Dordrecht, The Netherlands, 2014; pp. 393–424.
5. Santos, R.; Mello Junior, J.A.; Caraschi, J.C.; Ventorim, G.; Pereira, F.A. Polpacao kraft e kraft/Aq da madeira pre-hidrolisada de *Eucalyptus urograndis*. *Cienc. Florest.* **2016**, *26*, 1281–1290. [CrossRef]
6. Naidoo, S.; Kulheim, C.; Zwart, L.; Mangwanda, R.; Oates, C.N.; Visser, E.A.; Wilken, F.E.; Mamni, T.B.; Myburg, A.A. Uncovering the defence responses of Eucalyptus to pests and pathogens in the genomics age. *Tree Physiol.* **2014**, *34*, 931–943. Available online: http://www.treephys.oxfordjournals.org (accessed on 6 February 2020). [CrossRef]
7. Chauhan, S.S.; Walker, J. Relationships between longitudinal growth strain and some wood properties in *Eucalyptus nitens*. *Aust. For.* **2004**, *67*, 254–260. [CrossRef]
8. Blackburn, D.; Hamilton, M.; Harwood, C.; Innes, T.; Potts, B.; Williams, D. Stiffness and checking of *Eucalyptus nitens* sawn boards: Genetic variation and potential for genetic improvement. *Tree Genet. Genomes* **2010**, *6*, 757–765. [CrossRef]
9. Farrell, R.; Innes, T.C.; Harwood, C.E. Sorting *Eucalyptus nitens* plantation logs using acoustic wave velocity. *Aust. For.* **2012**, *75*, 22–30. [CrossRef]
10. Blackburn, D.; Farrell, F.; Hamilton, M.; Volker, P.; Harwood, C.; Williams, D.; Potts, B. Genetic improvement for pulpwood and peeled veneer in *Eucalyptus nitens*. *Can. J. For. Res.* **2012**, *42*. [CrossRef]
11. Gilbert, B.P.; Bailleres, H.; Zhang, H.; McGavin, R.L. Strength modelling of laminated veneer lumber (LVL) beams. *Constr. Build. Mater.* **2017**, *149*, 763–777. [CrossRef]
12. Bal, B.C. Some technological properties of laminated veneer lumber produced with fast-growing poplar and eucalyptus. *Maderas. Cienc. Tecnol.* **2016**, *18*, 413–424. [CrossRef]
13. Crafford, P.L.; Wessels, C.B. The potential of young, green finger-jointed *Eucalyptus grandis* lumber for roof truss manufacturing. *South. For. J. For. Sci.* **2016**, *78*, 61–71. [CrossRef]
14. Gilbert, B.P.; Underhill, I.D.; Bailleres, H.; El Hanandeh, A.; McGavin, R.L. Veneer based composite hollow utility poles manufactured from hardwood plantation thinned trees. *Constr. Build. Mater.* **2014**, *66*, 458–466. [CrossRef]
15. Deidda, A.; Buffa, F.; Linaldeddu, B.T.; Pinna, C.; Scanu, B.; Deiana, V.; Satta, A.; Franceschini, A.; Floris, I. Emerging pests and diseases threaten *Eucalyptus camaldulensis* plantations in Sardinia, Italy. *iForest Biogeosci. For.* **2016**, *9*, 883–891. [CrossRef]
16. Hashim, M.N.; Mohd Hazim, M.A.; Syafinie, A.M. Strategic forest plantation establishment in malaysia for future product development and utilisation. *Int. J. Agric. For. Plant.* **2015**, *1*, 14–24.
17. Branco, M.; Dhahri, S.; Santos, M.; Jamaa, M.L.B. Biological control reduces herbivore's host range. *Biol. Control.* **2014**, *69*, 59–64. [CrossRef]
18. Old, K.M.; Davison, E.M. Canker diseases of eucalypts. In *Diseases and Pathogens of Eucalypts*; Keane, P.J., Kile, G.A., Podger, F.D., Brown, B.N., Eds.; CSIRO Publishing: Collingwood, Australia, 2000; pp. 241–257.
19. Gryzenhout, M.; Myburg, H.; Van der Merwe, N.A.; Wingfield, B.D.; Wingfield, M.J. Chrysoporthe, a new genus to accommodate *Cryphonectria cubensis*. *Stud. Mycol.* **2004**, *50*, 119–142.
20. Old, K.M.; Wingfield, M.J.; Yuan, Z.Q. *A Manual of Diseases of Eucalypts in South-East Asia*; CIFOR: Jakarta, Indonesia, 2003.
21. Gezahgne, A.; Cortinas, M.N.; Wingfield, M.J.; Roux, J. Characterisation of the Coniothyrium stem canker pathogenon *Eucalyptus camaldulensisin* Ethiopia. *Australas. Plant Pathol.* **2005**, *34*, 85–90. [CrossRef]
22. Rauf, M.R.B.A.; McTaggart, A.R.; Marincowitz, S.; Barnes, I.; Japarudin, Y.; Wingfield, M.J. Pathogenicity of *Chrysoporthe deuterocubensis* and *Myrtoporthe bodenii* gen. et sp. nov. on Eucalyptus in Sabah, Malaysia. *Australas. Plant Pathol.* **2019**. [CrossRef]
23. Mafia, R.G.; Ferreira, M.A.; Zauza, A.V.; Silva, J.F.; Colodette, J.L.; Alfenas, A.C. Impact of *Ceratocystis* wilt on eucalyptus tree growth and cellulose pulp yield. *For. Path.* **2013**, *43*, 379–385. [CrossRef]
24. Davis, J.M.; Wu, H.; Cooke, J.E.; Reed, J.M.; Luce, K.S.; Michler, C.H. Pathogen challenge, salicylic acid, and jasmonic acid regulate expression of chitinase gene homologs in pine. *Mol. Plant Microbe Interact.* **2002**, *15*, 380–387. [CrossRef] [PubMed]
25. Muhammad, S.A.R. Isolation and Identification of Causal Disease of *Eucalyptus pellita*. Bachelor's Thesis, Universiti Malaysia Sarawak, Kota Samarahan, Malaysia, 2012.
26. Mohali, S.R.; Slippers, B.; Wingfield, M.J. Identification of botryosphaeriaceae from eucalyptus, acacia and pinus in Venezuela. *Fungal Divers.* **2007**, *25*, 103–125.
27. Burgess, T.I.; Barber, P.A.; Hardy, G.E.S. *Botryosphaeria* spp. associated with eucalypts in Western Australia, including the description of *Fusicoccum macroclavatum* sp. nov. *Austral. Plant Pathol.* **2005**, *34*, 557–567. [CrossRef]

28. Slippers, B.; Fourie, G.; Crous, P.W.; Coutinho, T.A.; Wingfield, B.D.; Carnegie, A.J.; Wingfield, M.J. Speciation and distribution of *Botryosphaeria* spp. on native and introduced eucalyptus trees in Australia and South Africa. *Stud. Mycol.* **2004**, *50*, 343–358.
29. Aylward, J.; Roets, F.; Dreyer, L.L.; Wingfield, M.J. Teratosphaeria stem canker of eucalyptus: Two pathogens, one devastating disease. *Mol. Plant Pathol.* **2019**, *20*, 8–19. [CrossRef]
30. Gezahgne, A. Main Diseases of Eucalyptus Species in Ethiopia. In *Eucaluptus Species Management, History, Status and Trends in Ethiopia*; Wubalem, G., Lopez, T., Eds.; Technical University of Madrid: Madrid, Spain, 2010; pp. 351–369.
31. Gezahgne, A.; Roux, J.; Thu, P.Q.; Wingfield, M.J. Coniothyrium stem canker of eucalyptus, new to Argentina and Vietnam. *S. Afr. J. Sci.* **2003**, *99*, 587–588.
32. Derikvand, M.; Kotlarewski, N.; Lee, M.; Jiao, H.; Nolan, G. Characterisation of physical and mechanical properties of unthinned and unpruned plantation-grown *Eucalyptus nitens* H. Deane & Maiden Lumber. *Forests* **2019**, *10*, 194. [CrossRef]
33. ISO 13061-1 (E). *Physical and Mechanical Properties of Wood-Test. Methods for Small Clear Specimens*; ISO: Geneva, Switzerland, 2014.
34. ISO 3347 (E). *Wood—Determination of Ultimate Shearing Stress Parallel to Grain*; ISO: Geneva, Switzerland, 2014.
35. BS 373. *Standard Test. Methods for Mechanical Properties of Lumber and Wood-Based Structural Material*; British Standard Institution: London, UK, 1957; ISBN 0580006840.
36. ASTM Standard D 143-09. *Standard Test Method for Small Clear Specimens of Timber*; ASTM International: West Conshohocken, PA, USA, 2009.
37. Gunduz, G.; Oral, M.A.; Akyuz, M.; Aydemir, D.; Yaman, B.; Asik, N.; Bulbul, A.S.; Allahverdiyev, S. Physical, morphological properties and raman spectroscopy of chestnut blight diseased *Castanea Sativa* Mill. wood. *CERNE* **2016**, *22*, 43–58. [CrossRef]
38. Alfenas, A.C.; Ferreira, M.A.; Mafia, R.G.; Zauza, E.A.V.; Binoti, D.H.B. Volume and Pulp Yield of Healthy and Infested Trees of *Eucalyptus urophylla* × *E. grandis* by *Ceratocystis fimbriata*. Available online: https://www.eucalyptus.com.br/artigos/outros/10A_Pest_effects.pdf (accessed on 8 November 2020).
39. Fernandes, B.V.; Zanuncio, A.J.V.; Furtado, E.L.; Andrade, H.B. Damage and loss due to *Ceratocystis fimbriata* in eucalyptus wood for charcoal production. "Eucalyptus fungal loss". *BioResources* **2014**, *9*, 5473–5479. [CrossRef]
40. Prasetyo, A.; Aiso, H.; Ishiguri, F.; Wahyudi, I.; Wijaya, I.P.G.; Ohshima, J.; Yokota, S. Variations on growth characteristics and wood properties of three eucalyptus species planted for pulpwood in Indonesia. *Tropics* **2017**, *26*, 59–69. [CrossRef]
41. Wessel, C.B.; Crafford, P.L.; Toit, B.D.; Grahn, T.; Johnsson, M.; Lundqvist, S.O.; Sall, H.; Seifert, T. Variation in physical and mechanical properties from three drought tolerant eucalyptus species grown on dry west coast of Southern Africa. *Eur. J. Wood Wood Prod.* **2016**, *74*, 563–575. [CrossRef]
42. Kothiyal, V.; Raturi, A.; Dubey, Y.M. Enhancing the applicability of near infrared spectroscopy for estimating specific gravity of green timber from *Eucalyptus tereticornis* by developing composite calibration using both radial and tangential face of wood. *Eur. J. Wood Wood Prod.* **2014**, *72*, 11–20. [CrossRef]
43. Hein, P.R.G.; Silva, J.R.M.; Brancheriau, L. Correlation among microfibril angle, density, modulus of rupture and shrinkage in 6-year–old *Eucalyptus urophylla* × *E. grandis*. *Maderas Cienc. Technol.* **2013**, *15*, 171–182. [CrossRef]
44. Medhurst, J.; Downes, G.; Ottenschlaeger, M.; Harwood, C.; Evans, R.; Beadle, C. Intra-specific competition and the radial development of wood density, microfibril angle and modulus of elasticity in plantation-grown *Eucalyptus nitens*. *Trees* **2012**, *26*, 1771–1780. [CrossRef]
45. Schwarze, F.W.M.R.; Engels, J.; Mattheck, C. *Fungal Strategies of Wood Decay in Trees*; Springer: Berlin/Heidelberg, Germany, 2000.
46. Rasdianah, D.; Lee, S.H.; Zaidon, A.; Edi, S.B.; Hidayah, A.; Khoo, P.S.; Paiman, B.; Qamariah, N.S. Durability of superheated steam-treated light red meranti (*Shorea* spp.) and kedondong (*Canarium* spp.) wood against white rot fungus and subterranean termite. *Sustainability* **2020**, *12*, 4431. [CrossRef]
47. Acosta, M.S.; Concordia, E.R.; Mastrandrea, A.C.; Lima, A.J.T. Wood technologies and uses of Eucalyptus from fast grown plantation for solid products. In Proceedings of the 51st International Convention of Society of Wood Science and Technology, Concepción, Chile, 10–12 November 2008.
48. Wilcox, W.W. Review of literature on the effects of early stages of decay on wood strength. The society of wood science and technology. *Wood Fiber.* **1978**, *9*, 252–257.
49. Pima, N.E.; Iddi, S.; Chamshama, S.A.O.; Maguzu, J. Wood properties of eucalyptus hybrid clones growing in Tanzania. *Int. J. Agric. For.* **2018**, *8*, 220–226. [CrossRef]
50. Blanchette, R.A.; Nilsson, T.; Daniel, G.; Abad, A. Biological Degradation of Wood. In *Archaeological Wood*; Rowell, R.M., Babour, R.J., Eds.; American Chemical Society: Washington, WA, USA, 1990. [CrossRef]
51. Salmiah, U.; Andrew, H.H.W.; Jones, E.B.G. Wood degrading fungi. In *Malaysian Fungal Diversity*, 1st ed.; Jones, E.B.G., Hyde, K.D., Vikneswary, S., Eds.; Mushroom Research Centre, University of Malaya & Ministry of Natural Resources and Environment: Kuala Lumpur, Malaysia, 2007.
52. Gordh, G.; Mckirdy, S. *The Handbook of Plant Biosecurity*; Springer: New York, NY, USA, 2014.
53. Baker, M.C. CBD-111. Decay of wood. National Research Council Canada/ Institute for research in construction. *Can. Build. Dig. Publ.* **1969**.
54. Bodig, J.; Jayne, B.A. *Mechanics of Wood and Wood Composites*; Van Nostrand Reinhold: New York, NY, USA, 1982.